Article

Augmenting vaccine immunogenicity through the use of natural human anti-rhamnose antibodies

Md Kamal Hossain, Abhishek Vartak, Partha Karmakar, Steven J. Sucheck, and Katherine A. Wall

ACS Chem. Biol., **Just Accepted Manuscript** • DOI: 10.1021/acschembio.8b00312 • Publication Date (Web): 19 Jun 2018

Augmenting vaccine immunogenicity through the use of natural human anti-rhamnose antibodies

Md Kamal Hossain[1], Abhishek Vartak[2], Partha Karmakar[2], Steven J. Sucheck[2], Katherine A. Wall[1*]

1. *Dept. of Medicinal and Biological Chemistry, University of Toledo, Toledo, OH.*
2. *Dept. of Chemistry and Biochemistry, University of Toledo, Toledo, OH.*

Abstract

Utilizing natural antibodies to augment vaccine immunogenicity is a promising approach towards cancer immunotherapy. Anti-rhamnose (anti-Rha) antibodies are some of the most common natural anti-carbohydrate antibodies present in human serum. Therefore, rhamnose can be utilized as a targeting moiety for a rhamnose-containing vaccine to prepare an effective vaccine formulation. It was shown previously that anti-Rha antibody generated in mice binds effectively with Rha-conjugated vaccine and is picked up by antigen presenting cells (APCs) through stimulatory Fc receptors. This leads to the effective uptake and processing of antigen and eventually presentation by major histocompatibility complex (MHC) molecules. In this article, we show that natural human anti-Rha antibodies can also be used in a similar mechanism and immunogenicity can be enhanced by targeting Rha-conjugated antigens. In doing so, we have purified human anti-Rha antibody from human serum using a rhamnose affinity column. *In vitro*, human anti-Rha antibodies are shown to enhance the uptake of a model antigen, Rha-ovalbumin (Rha-Ova), by APCs. In-vivo, they improved the priming of CD4+ T cells to Rha-Ova in comparison to non-anti-Rha human antibodies. Additionally, increased priming of both CD4+ and CD8+ T cells towards the cancer antigen MUC1-Tn was observed in mice that received human anti-Rha antibodies prior to vaccination with a rhamnose-modified MUC1-Tn cancer vaccine. The vaccine conjugate contained Pam_3CysSK_4, a Toll-like receptor (TLR) agonist linked via copper-free cycloaddition chemistry to a 20-amino-acid glycopeptide derived from the tumor marker MUC-1 containing the tumor-associated carbohydrate antigen α-*N*-acetyl galactosamine (GalNAc). The primed CD8+ T cells released IFN-γ and killed tumor cells. Therefore, we have confirmed that human anti-Rha antibodies can be effectively utilized as a targeting moiety for making an effective vaccine.

Keywords: Anti-rhamnose antibodies, human serum, APCs, Fc receptors, CD4+ T cells, CD8+ T cells, Rha-Ova, MUC1-Tn.

*Correspondence: katherine.wall@utoledo.edu

Introduction

Vaccination is a promising approach towards cancer immunotherapy. The prime goal of its use is to produce both cancer-specific humoral and cellular immunity [1]. To elicit a strong protective immune response, a vaccine construct has to be processed and presented by antigen presenting cells (APCs) such as dendritic cells or macrophages. These cells, especially dendritic cells, have the unique ability to generate both primary and secondary anti-tumor immune responses [2-4]. After capturing antigens, APCs transport them to regional lymph nodes where naive T cells can encounter a cognate antigen for their activation. Antigens are processed and presented on Class I and Class II major histocompatibility complex (MHC) molecules for CD8+ and CD4+ T cell activation [5-8]. A weak immune response is correlated with poor uptake and presentation by APCs [9, 10]. Therefore, enhancement of antigen presentation is helpful for effective vaccine preparation.

One effective avenue of enhancement is an antibody-dependent antigen uptake mechanism by targeting Fc_Y receptors on APCs that can bind with the Fc portion of an immune complexed (Ag-IgG) antibody [10, 11]. This Fc_Y-FcR interaction induces the internalization of the vaccine, maturation of DCs, and better presentation on MHC Class I and Class II molecules. When incubated with dendritic cells, this immune complex induces a maturation signal that enables dendritic cells to prime antigen-specific CD8+ T cells independently of CD4+ T helper cells and receive a 'license to kill' signal [12]. This proves that the antibody can induce a cytotoxic T cell response.

Glycoconjugate expression on cancer cells is aberrant and found in abnormal quantities compared to glycoconjugates found on normal cells [13]. The unique structural modification and overexpression of carbohydrate epitopes on cancerous cells make them attractive targets for a tumor vaccine. These tumor-associated carbohydrate antigens (TACA) are thought to stimulate production of antibodies which are correlated with increased survival [14]. However, they are known to elicit a T cell-independent immune response and are not able to switch the isotype from IgM to IgG without further help and therefore they are only weakly immunogenic [15, 16]. They do not usually activate T helper cells by themselves and thus produce low-affinity IgG and IgM antibodies. A number of TACAs, including Tn, TF, and STn, are found on MUC1, a large polymorphic transmembrane glycoprotein [17-20]. MUC1 contains numerous 20 amino acid long variable number tandem repeats and is generally found on the apical surface of normal glandular epithelia [21, 22]. In order to increase the immunogenicity, TACAs have been conjugated with different carrier proteins e.g., bovine serum albumin (BSA), ovalbumin (Ova) or keyhole limpet hemocyanin to break the immune tolerance to the structures [23-25]. Peptides from the carrier proteins are expected to bind with MHC class II and stimulate CD4+ T cells to provide help for antibody class switching from IgM to IgG. However, the problem with carrier proteins is that they are themselves immunogenic and an immune response against those proteins can impede the response to the carbohydrate epitope [26, 27]. Also, these carrier-primed T cells cannot recognize tumor antigens to be restimulated by the tumor following immunization. In order to further increase the vaccine immunogenicity and to obtain a higher IgG titer, an immunostimulatory adjuvant can also be used along with the TACA [28]. In our studies, we used a

TLR2 agonist, Pam_3CysSK_4 as an immunostimulatory adjuvant that can facilitate DC maturation and better presentation of antigen to T cells.

Targeting natural antibodies to exploit the immune system for killing tumor cells is a promising approach in the anti-tumor strategy. Natural antibodies found in humans are mostly IgM, IgG3, and IgA [29]. Generally, they are able to recognize self-antigens through their V regions and lack specificity to recognize any particular foreign antigen. Recent high throughput studies on human serum have recognized some high-titer natural antibodies that are specific to some carbohydrate epitopes [30]. Some of the most abundant antibodies found in human serum are against α-gal, L-Rha, and different blood group antigens. Among them, anti-Rha antibody is present in a higher quantity in human serum. Because of its higher abundance and capacity to form complexes with its epitope L-Rha, anti-Rha antibody is considered as an attractive option for targeted immunotherapy [31-33].

Our labs have previously shown that the effectiveness of a cancer vaccine could be increased by conjugation of a helper T-cell peptide and a B-cell antigen with an L-rhamnose (Rha) carbohydrate epitope [31, 34, 35]. This exploits the antibody-mediated antigen uptake mechanism used by Galili et al. for the α-gal epitope. The α-gal antibody, a natural antibody found in human serum, formed immune complexes with the α-Gal epitope in order to boost immune responses [36, 37]. However, it has been found that anti-Rha antibody, a natural antibody against L-rhamnose, is even more abundant than α-Gal antibody in human serum [30]. Also, these antibodies are highly antigen-specific and present in high titers in human serum samples. The hypothesis is that the Fc portion of the anti-Rha IgG or IgM antibody complexed with the Rha-conjugated vaccine, can be recognized by Fcγ receptors or other receptors on APCs such as dendritic cells. This results in an overall internalization of the vaccine and better presentation on the human or mouse MHC. This has been shown by generating anti-Rha antibodies in mice by immunizing with Rha-Ficoll [34]. This led us to ask if human anti-Rha antibodies, isolated from pooled human serum also enhance immune responses in mice and therefore hopefully also in humans. In these studies, we have used two Rha-conjugated antigens to examine enhancement both *in vitro* and *in vivo*. We have used previously synthesized Rha-Ova as a model antigen [31, 35]. A newly synthesized liposomal Rha-conjugated vaccine (Pam_3CysSK_4-DBCO-MUC1-Tn) was used to target with human anti-Rha antibodies.

Results

Purification and Characterization of Human Anti-rhamnose Antibodies

To examine the presence of human anti-Rha antibody in human serum, a rhamnose specific ELISA was performed with pooled human serum. High titers of anti-Rha antibodies reacting with both anti-human IgG and IgM antibodies show that human serum contains a considerable amount of both anti-Rha IgG and anti-Rha IgM (Fig. 1A). Our next step was to purify human anti-Rha antibodies from human serum using a rhamnose affinity column. Commercially available CNBr-activated Sepharose was conjugated with previously synthesized rhamnose-2 aminoethyl linker to prepare the column [35]. Pooled human serum samples were then passed through the column. Only anti-Rha antibody should bind to the column whereas unbound

antibodies should pass through. This 'pass through' solution contained all other human antibodies except anti-rhamnose antibody and hence was used as a control in most of the following studies. The pass through was brought to 40% (w/v) ammonium sulfate and the precipitate was dialyzed to yield enriched immunoglobulins. An ELISA assay of the samples collected from different steps of affinity column chromatography purification showed the existence of purified anti-rhamnose antibody (Fig. 1B). A significant amount of purified anti-Rha antibodies eluted when 100 mM rhamnose solution was applied to the column. The low activity in the other fractions demonstrates that almost all anti-Rha antibodies are represented in the 100 mM rhamnose eluate.

Additionally, a rhamnose specific ELISA on the antibodies before and after purification showed that most of the anti-rhamnose antibodies are IgM and some of them are IgG1 and IgG3. Our purified antibodies also reflect this distribution (Fig. 1C & 1D).

Enhancement of Antigen Presentation Occurs when Rha-Ova is Targeted by Human Anti-Rha Antibody

To determine whether human anti-Rha antibody binds with the rhamnose modified Rha-Ova and helps in an antibody-dependent antigen uptake mechanism, an *in vitro* CD4+ proliferation assay was performed with ovalbumin-primed mouse CD4+ T cells. Two mice were immunized with ovalbumin. After seven days, mice were sacrificed and CD4+ T cells were purified from the spleen cell suspension. A CD4+ T cell proliferation assay was performed to determine whether ovalbumin specific CD4+ T cells proliferate more when added to murine bone marrow-derived dendritic cells (DCs) incubated with human anti-Rha antibody and different concentrations of Rha-Ova. Pass through antibodies, that contain other human antibodies except anti-Rha antibodies, were used as a control. As predicted, enhanced T cell proliferation was observed with increasing concentrations of Rha-Ova (Figure 2A). CD4+ T cells proliferated more than twice as much in the presence of human anti-Rha antibodies compared to the other two groups.

In order to determine the antigen presentation enhancement ability of human anti-Rha antibodies *in vivo*, three groups of six C57BL/6 mice were injected with purified antibodies, pass through or PBS. After one hour, all the mice were immunized with Rha-Ova. A week later, mice were sacrificed and spleen cell suspensions were prepared. CD4+ T cells were separated and T cell priming was tested by proliferation in the presence of DCs and different concentrations of ovalbumin. CD4+ T cell priming as indicated by proliferation was more in the anti-Rha antibody group compared to the control group (pass through antibody) (Fig. 2B & 2C).

Antigen Presentation Enhancement by Anti-Rha IgG and IgM is Comparable to the Unseparated Anti-Rha Antibody

To better understand the isotype of anti-Rha antibodies that are responsible for the uptake enhancement, anti-Rha IgG antibody was separated from anti-Rha IgM using protein G affinity column chromatography. Western blotting was performed to confirm the separation of IgG and IgM antibodies. This shows that both anti-Rha IgG and IgM were separated and without contamination by the other (Fig. S1).

To determine whether anti-Rha IgG or anti-Rha IgM or both are responsible for uptake enhancement, an *in vitro* CD4+ T cell proliferation assay was performed. Two mice were immunized with ovalbumin to produce Ova primed CD4+ T cells and sacrificed at day 21 to separate CD4+ T cells from the spleen. CD4+ T cell proliferation was assayed in the presence of DCs, Rha-Ova and each of the separated antibodies and compared with the pass through antibody. Dendritic cells enhanced the proliferation of CD4+ T cells in groups that contained anti-Rha, anti-Rha IgG and anti-Rha IgM antibody compared to the pass through group (Fig. 3) and no antibody.

Immunization with Rha-ova elicits Ova specific antibody:

The *in vivo* antigen enhancement ability of different separated anti-Rha antibodies was also examined. A total of 18 mice were distributed in five groups with 4 mice in each group except group E which was used as background. Four groups of mice received the respective antibody first whereas the last group received PBS only. The first group received unfractionated anti-Rha antibody (10 μg) whereas the second and third groups received the equivalent amount of either anti-Rha IgG (2 μg) or anti-Rha IgM (8 μg) separated from whole anti-Rha antibody. After one hour, all mice received Rha-Ova (40 μg per mouse).

All mice were bled and sacrificed at day 7. Anti-Ova antibody production was determined on an ovalbumin coated plate. Mice that received either unfractionated anti-Rha or anti-Rha IgG antibody generated higher antibody titers. Interestingly, mice receiving anti-Rha IgM produced little more anti-Ova antibody in comparison to mice receiving Rha-Ova alone (Fig. 4A). These results could be interpreted to show that the first two groups of mice had produced more primed helper T cells that help B cells to produce an antibody that is specific to Ova antigen than the group that received anti-Rha IgM.

Helper CD4+ T cell proliferation assay, *in vivo*:

In order to analyze helper CD4+ T cell priming *in vivo* in the presence of different purified antibodies, CD4+ T cells were separated from the spleens of those mice and an antigen (Ova) dependent proliferative response was determined in the presence of DCs. The highest proliferation was observed in the presence of Ova (10^{-6} M) (Fig. 4B). At this concentration, CD4+ T cells from the anti-Rha treated group proliferated most. The anti-Rha IgM and anti-Rha IgG treated groups also showed increased proliferation in comparison to the control group, suggesting that both of the antibodies bound with Rha-conjugated antigen (Rha-Ova) which was more efficiently picked up by APCs (Fig. 4C). This suggests that the lack of enhancement of anti-Ova antibody production by anti-Rha IgM observed above is not due to reduced helper T cell priming.

Mixed-phase synthesis of Pam_3CysSK_4 (Compound 5)

The importance of immuno-adjuvant in carbohydrate-based vaccines is well established [38]. Their role in improved antigen processing and presentation and maturation of DC's is evident from the literature [39]. Pam_3CysSK_4, a synthetic lipopeptide and TLR-2/1 ligand, was utilized for this purpose. Upon activation, TLR lead to pro-inflammatory cytokines via NF-kB transcription

factor activation [40]. The peptide portion of the molecule, SK_4 was synthesized by solid phase peptide synthesis (SPPS) using Fmoc strategy (Fig. 5). 2-Chlorotrityl chloride resin was used for SPPS as it is more acid labile and peptide cleavage from the resin can be achieved with the treatment by an acetic acid: DCM mixture without de-protecting the amino acid side-chains. Loading of the first amino acid on the resin was achieved in the presence of DIPEA and N_α-Fmoc-N_ε-Boc-L-lysine. The capping of free sites on the resin after loading was ensured by addition of methanol. A mixture of 25% piperidine in DMF was used for Fmoc deprotection and the resin bound coupling was performed using DIC and HOBt and was monitored using the ninhydrin test. After every reaction, resin beads were thoroughly washed with DCM and DMF. Compound **1** (Scheme 1, Fig. 5) was prepared as previously reported from L-Cystine bis(*tert*-butyl ester) dihydrochloride with 69.5% yield over 3 steps [41]. Fmoc de-protection of **1** using diethylamine followed by coupling with palmitic acid in the presence of coupling reagent PyBOP, HOBt afforded compound **2** with 71% yield. Compound **2** on de-protection in the presence of a TFA:DCM mixture resulted in compound **3** with quantitative yield (**Scheme 1**). *S*-((*R*)-2,3-bis(palmitoyloxy)propyl)-*N*-palmitoyl-L-cysteine (**3**) was then coupled with side-chain protected SK_4 on the solid phase to achieve resin bound Pam_3CysSK_4. The resin beads were filtered off after acetic acid treatment to obtain compound **5** with an overall yield of 33%.

Synthesis of Pam_3CysSK_4 -DBCO-MUC1 VNTR-TACA conjugate (Compound 9)

Compound **5** was coupled with the amine-terminated, strained alkyne derivative azadibenzocyclooctyne-amine (DBCO-amine) in the presence of propyl phosphonic anhydride (T_3P) to afford alkyne-terminated immuno-adjuvant component **6** (**Scheme 2**). Compound **7**, an azide terminated human MUC1 variable number tandem repeat (VNTR) containing Tn as tumor-associated carbohydrate antigen (TACA) was prepared as previously reported [35]. The antigenic sequence contains $CD8^+$ as well as $CD4^+$ T cell epitopes. The azide terminated antigen (**7**) was stirred with strained alkyne component **6** in MeOH:DCM mixture under N_2 at RT (**Scheme 3**). The reaction was monitored by MALDI and was observed complete after 12 h. The side-chain de-protection was done using TFA cleavage cocktail (DCM:TFA:TES) and the final cyclo-addition product **9** was precipitated out of cold ether.

Synthesis of Rha-TEG-Cholesterol

Rha-TEG-Cholesterol was synthesized as previously described and used in the formulation of liposomes [34].

Enhanced Uptake of a Cancer Antigen (MUC1-Tn) Using Human Anti-Rha Antibodies *in vivo*

We next sought to determine the antigen presentation enhancement abilities of human anti-Rha antibody in the presence of Rha-conjugated cancer vaccine Pam_3CysSK_4-DBCO-MUC1-Tn. The immunization concept utilized here was the same as with the model antigen Rha-Ova. Three batches of liposomal formulations were prepared. Stock solutions were prepared of DPPC, cholesterol, and Rha-TEG-Cholesterol. Aliquots from stock solutions were mixed to obtain a lipid solution of 30 mM in a total volume of 2 mL. The first batch contained Pam_3CysSK_4 -DBCO-MUC1 VNTR-TACA conjugate **9** (0.2 μmoles), Cholesterol-TEG-Rha (10%),

cholesterol (10%) and DPPC (80%). The second batch contained Pam_3CysSK_4 -DBCO-MUC1 VNTR-TACA conjugate **9** (0.2 μmoles)**,** DPPC (80%) and cholesterol (20%) and the third batch contained only DPPC (80%) and cholesterol (20%). All the liposomes were formulated by the extrusion method with 100 nm polycarbonate membrane as previously described [34].

Fifteen female mice were subdivided into 5 different groups and received one priming and three boosts at 14 day intervals (Day, 0, 14, 28, 42). They received either anti-Rha antibody (Groups A-B) or pass through antibody (Groups C-D) except group E which received only blank liposomes. After one hour, the first four groups of mice were immunized each with 100 μl of cancer vaccines (10 nmoles of Pam_3CysSK_4-MUC1-Tn) with or without rhamnose.

Anti-Rha Antibody and Rha-Vaccine Immunized Mice Produce More Anti-MUC1-Tn Antibody

Seven days after the 2nd boost, mice were bled for serum separation. An ELISA assay was performed to measure anti-MUC1-Tn antibody production by screening mice sera on plates coated with previously synthesized MUC1-Tn [34]. As predicted, anti-MUC1-Tn antibody titer was highest in group A compared to the other three groups (Blank liposome values were considered as background and subtracted.) (Fig. 6A). The other three groups also elicited anti-MUC1-Tn antibody titers, since they were also immunized with MUC1-Tn vaccines but the titers were lower. This shows that human anti-Rha antibody can be utilized to enhance uptake and processing of a glycoprotein antigen by DCs.

Enhanced Uptake Leads to Enhanced CD4+ T cell Priming

A CD4+ T cell proliferation assay was performed to determine if targeting with human anti-Rha antibodies helps in the generation of MUC1-Tn primed CD4+ T cells. The proliferation of CD4+ T cells was measured with varying concentrations of MUC1-Tn antigen and DCs. The data showed that CD4+ T cells proliferated in a concentration-dependent manner, with maximal proliferation at 20 μg mL^{-1} MUC1-Tn antigens (Fig. 6B). At this concentration, CD4+ T cells from group A proliferated significantly more compared to cells from groups B-D (Fig. 6C), indicating more effective priming *in vivo*.

Enhanced Cross-presentation Leads to Enhanced CD8+ T cell Priming

Tumor-specific cytotoxic T lymphocytes (CTL) are very crucial for effective cancer immunotherapy. Cross-presentation is required for efficient capture and presentation of external antigens to CD8+ T cells via MHC class I molecules. Therefore, inducing a strong CD8+ T cell response is a challenge for tumor vaccines. CD8+ T cell priming in the different groups was examined to DCs in the presence of previously synthesized and reported CD8+ T cell epitope SAPDTnRPA [35]. Concentration-dependent proliferation shows 40 μg mL^{-1} of the short peptide was the minimum concentration needed for effective stimulation in group A (Fig. 7A). Anti-Rha antibody helped in effective capture and cross-presentation of antigen on MHC I, as shown by the enhanced proliferation of CD8+ T cells from group A compared to the other three groups (Groups B-D) (Fig. 7B). In group B, despite the presence of anti-Rha antibody during priming, CD8+ T cells did not proliferate better due to the absence of rhamnose on the vaccine. Similarly,

group C and D mice showed less CD8+ T cell proliferation due to the absence of anti-Rha antibody.

CD8+ T Cells Release More IFNγ after Priming in the Presence of Human Anti-Rha Antibody

IFNγ secretion by CD8+ T cells was measured by incubating primed CD8+ T cells from the previously described groups of mice along with dendritic cells and the CD8+ T cell epitope. IFNγ secretion was measured by ELISA to evaluate if enhanced uptake and presentation of vaccine to CD8+ T cells leads to more IFNγ secretion. It was found that IFNγ secretion was higher in the anti-Rha receiving group A compared to the other three groups since it has more educated CD8+ T cells that release IFNγ when restimulated (Fig. 7C).

Enhanced Cross-presentation Leads to the Enhanced Killing of Cancer Cells

The apoptosis-inducing ability of CD8+ cytotoxic T lymphocytes from the different groups was also determined using a JAM assay. A mouse lymphoma cell line (EL4) pulsed with the CD8+ T cell epitope was used as the target. It was found that CD8+ T cells from group A had increased capacity to kill pulsed EL4 cells compared to the other groups (Fig. 7D).

Discussion

Vaccine immunogenicity enhancement largely depends on efficient uptake and processing of antigen by APCs such as DCs and its successful presentation to T cells. Once DCs enter into the spleen and lymph node and activate B and T cells, they act as a channel to link innate and adaptive immunity. DCs have the ability to present processed exogenous antigen to CD4+ T cells via MHC II molecules and to CD8+ T cells via MHC I molecules through a process called cross presentation [42]. Enhanced immunogenicity to eliminate cancerous cells can be achieved by harnessing the immune effector function of natural antibody by including antibody recruiting molecules (ARMs) [32]. Binding of natural antibodies to the ARMs enhances uptake and antigen processing by DCs. Since human serum contains a large number of natural antibodies, different antibody targeting molecules have been used before to target those natural antibodies. Some of the popular ARMs include i.e. dinitrophenyl (DNP), galactose-α-1,3-galactose (α-gal) and L-Rhamnose [30, 43-45].

Our group has previously reported that anti-Rha antibody could be generated in non-transgenic mice and used as a targeting moiety for a rhamnose containing vaccine [31]. This resulted in efficient uptake and processing of vaccine antigen and better presentation to T cells through the MHC molecules of antigen presenting cells (APCs). The ultimate goal was to demonstrate that naturally occurring human anti-Rha antibody could also be used as a targeting molecule for generating a more effective vaccine.

The first aim of this study was to purify and analyze the natural anti-Rha antibodies in human serum. Affinity purified human anti-Rha and pass through control antibodies were used to target a rhamnose-containing model antigen (Rha-Ova) and compared CD4+ T cell proliferation, both *in vitro* and *in vivo*. More proliferation of Ova-primed T cells to DCs incubated with Rha-Ova in

the presence of anti-Rha antibodies confirmed that enhanced presentation of antigen was one mechanism of enhancement. Enhanced priming of anti-Ova CD4+ T cells demonstrated that human anti-Rha antibodies could encounter the vaccine in vivo, interact with murine APCs, and increase the anti-Ova response. Enhancement was observed even though the antigen was given with a strong adjuvant (Sigma adjuvant system).

Human serum and purified anti-Rha antibodies both contained abundant anti-Rha IgM, as well as Anti-Rha IgG1 and anti-Rha IgG3. This isotype distribution agrees with that observed previously in serum [32]. Anti-Rha IgG and anti-Rha IgM separately added to cultures in the same relative amounts as in the unseparated antibodies were also found to give improved proliferation of anti-Ova CD4+ T cells. Interestingly, anti-Ova antibody production was lower in the anti-Rha IgM group compared to anti-Rha and anti-Rha IgG antibody-receiving groups. This suggested that the other two groups of mice had produced more primed helper T cells that help B cells to produce anti-Ova Ab than the group that received anti-Rha IgM. However, proliferation studies showed equivalent priming of CD4+ T cells. These results show that receptors other than Fcγ receptors, possibly Fcμ or complement receptors, can participate in enhanced uptake and presentation of antigens bound to natural antibodies and subsequent T cell priming. However, the distribution of stimulatory and inhibitory receptors on different APCs and B cells may influence the amount of enhancement of different aspects of the immune response. Follow-up studies may examine the priming of B cells with the different enhancing antibodies, since our current studies have focused mostly on T cells.

Anti-Rha antibodies were also targeted to a rhamnose bearing liposomal cancer vaccine (MUC-Tn) to determine the possible enhancement of antigen presentation. Enhanced CD4+ T cell proliferation was found in the rhamnose-bearing liposomal cancer vaccine group given anti-Rha antibodies. Proliferation was much lower in the non-Rha liposomal vaccine group even though this group of mice also received anti-Rha antibodies. Similarly, targeting both rhamnose and non-rhamnose bearing liposomal vaccines with human pass though antibodies did not enhance T cell priming. Here, pass through antibodies contain all the antibodies from human serum except anti-Rha antibodies. These results demonstrate that a passive transfer approach can be used in mice to test vaccine responses utilizing natural antibodies, and that it is not necessary to generate murine natural antibody mimics.

Obtaining effector CD8+ T cells in addition to helper CD4+ T cells is now thought to be crucial in tumor eradication [46, 47]. Natural antibodies and complement have been shown to help enhance CD8+ T cell priming [48]. Therefore, CD8+ T cell priming was assessed in the vaccinated groups discussed above. The greatest CD8+ T cell proliferation was found in the rhamnose-bearing vaccine group given anti-Rha antibodies. The other three groups showed little CD8+ T cell priming, showing that this approach could be beneficial in order to enhance antigen presentation to CD8+ T cells through cross presentation. These activated CD8+ T cells were also found to have increased capacity to secrete IFN-γ in response to tumor antigen-pulsed DCs and enhanced cytotoxicity to tumor-antigen pulsed tumor cells. Overall, human anti-Rha antibodies gave similar enhancement of CD4+ and CD8+ T cell proliferation and function to that found with

murine anti-Rha antibodies [34, 35]. Enhancement of anti-MUC1-Tn antibody was less robust than observed with murine antibodies; however, anti-Ova antibodies showed more enhancement.

An advantage to using Rha as a targeting ligand for TACA vaccines is that we do not expect to shift the vaccine response towards the Rha carbohydrate and away from the TACA. Natural antibodies present in non-immunized individuals, such as the anti-Rha antibodies found in human serum, are mostly made by B-1 cells, a subset of B cells that do not display affinity maturation or produce a strong B cell memory [49].This means that the anti-Rha response to the vaccine would not be likely to dominate the response. In our previous studies using anti-Rha producing mice, we found that boosting mice with a Rha-conjugated vaccine did not increase the level of anti-Rha antibodies in the mice [31]. Therefore, natural antibody targeting with human anti-rhamnose antibodies is promising for generating anti-tumor responses that bring the entire spectrum of immune responses to bear on the tumor. Future experiments will examine the vaccine in environments that utilize human Fc receptors to enhance the immune responses.

Experimental procedures

Mouse immunization and human serum

Female C57BL/6 mice (7 to 8 weeks of age) were obtained from Jackson Laboratory, Bar Harbor, ME. Mice were injected with human antibodies as indicated and one hour later some mice were immunized with 40 μg of Rha-Ova in PBS emulsified with Sigma adjuvant system (SAS), 100 μl intraperitoneally (i.p.). One hour after antibody injection, other mice were injected i.p. with different liposomal formulations of a cancer vaccine with or without rhamnose, 100 μl containing 10 nmoles of Pam3CysSK4-MUC1-Tn antigen. All mice were maintained in the animal facility at the University of Toledo Health Science Campus under a specific pathogen-free environment. All mouse experiments were performed according to NIH guidelines with approval of the Institutional Animal Care and Use Committee. Pooled human serum was obtained from Zenbio, Inc.

ELISA assay

An ELISA assay was performed with pooled human serum for determining the presence of human anti-Rha antibody. A 96 well Immulon 4HBX plate was coated with previously synthesized Rha-BSA (2 μg mL^{-1}) [31] or BSA (2 μg mL^{-1}) from Sigma Aldrich in PBS overnight. The plate was then washed 5 times with washing buffer (PBS, 0.1% Tween-20), blocked with BSA in PBS (2 mg mL^{-1}) for 2 hours at room temperature, and washed 5 more times. Dilutions of human serum or purified antibody were added to the plate and incubated for an hour at room temperature. Following 5 more washes, HRP conjugated anti-human IgG or IgM was added at 1:2000 dilution. After 5 more washes, HRP one component TMB substrate (BioFX Lab.) was added. After 15-20 min, absorbance was recorded at 620 nm. The same procedures were followed for the determination of the presence of anti-Rha antibodies from different steps of column purification.

For measuring anti-Ova antibody production, the wells were coated with ovalbumin in PBS (4 μg mL^{-1}) and HRP goat anti-mouse IgG (H+L) (Invitrogen) at 1:10000 was used as the secondary antibody.

Anti-MUC1 antibody titer was measured by coating a 96 well plate with MUC1-Tn antigen (15 μg/mL in PBS) as above and using goat anti-mouse IgG (H+L) as secondary antibody.

Preparation of Rha affinity column for purifying anti-rhamnose antibody

A rhamnose affinity column was prepared by conjugating CNBr-activated Sepharose (Sigma-Aldrich) with rhamnose-2 aminoethyl linker [35]. One g of CNBr-activated Sepharose was added into 30 mL of 1 mM HCl for 15 minutes in a sintered glass filter. After repeating this process for 5-6 times and adding 7 mL of coupling buffer (0.1 M $NaHCO_3$, pH 8.3, 0.5 M NaCl), 2 mg (10 mL of 200 μg mL^{-1}) of rhamnose-2 aminoethyl linker solution was added and mixed in an end-over-end mixer for 2 hours at RT followed by centrifugation at 2000 rcf for 5 minutes. Supernatants were preserved for TNBS assay. Any remaining active groups were blocked by 15 mL of 1 M ethanolamine incubation for 2 hours. Following centrifugation, 15 mL of coupling buffer was added to the pellet and incubated for 10 minutes. After repeating the centrifugation and removing the supernatant, 15 mL of 0.1M sodium acetate buffer pH 4 containing 0.5 M NaCl was added. Next, 10 mL of coupling buffer was added to the resin. The washing was repeated at least 5 times with coupling buffer. TNBS assay confirmed quantitative coupling to the resin. The linker-Sepharose conjugate was poured into a column (1.5 x 10 cm) for purification of anti-rhamnose antibodies.

Separation of IgG using Protein G Sepharose 4B beads

Sixty μl of protein G Sepharose beads (Invitrogen) were centrifuged at 3700 rpm for 2 min and the supernatant was removed. Twenty five μg of anti-Rha antibody in 500 μl was added and incubated overnight at 4˚C. The samples were centrifuged at 3700 rpm for another 2 min and separated. The supernatant containing IgM was removed. Two hundred μl of Gly-HCl (0.1 M, pH 2.5) was added to the pellet and incubated for 10 min. After centrifugation, the supernatant was collected and 100 μl 1 M Tris-HCl pH 8.3 was added to neutralize it. The sample was dialyzed against 1 L PBS two to three times.

Western blotting

Isolated antibodies (anti-Rha IgG or anti-Rha IgM) were mixed with loading dye and boiled for 15 min. Those were then loaded into a 10% polyacrylamide gel for electrophoretic separation. The gel was transferred to a PVDF membrane and subsequently blocked with 25 mL of 5% w/v nonfat dry milk in Tris-buffered saline with 0.1% (v/v) Tween-20 (TBS/T) for 1 hr at room temperature. After 3 washes with TBS/T, membranes were incubated overnight at 4˚C with 10 mL of HRP conjugated anti-human IgG-Fc specific or anti-human IgM-μ chain specific antibodies at a dilution of 1:25000. After 3 washes, membranes were exposed to BioRad ECL Western substrate and the image was taken on a ChemiDoc Imaging System (BioRad).

Spleen cell suspension preparation

Mice were euthanized using CO_2 followed by cervical dislocation. Spleen cells were collected by passage through a 70 μ nylon mesh in 5 mL of T cell media (RPMI 1640 with L-glutamine, 10% heat inactivated fetal bovine serum, 5 x 10^{-5} M β-mercaptoethanol, 2 mM L-glutamine, 20 mM HEPES pH 7.4, 100 U mL^{-1} penicillin, 100 μg mL^{-1} streptomycin, and 1% media additions (0.06 g folic acid, 0.36 g L-asparagine, 1.16 g L-arginine, 2.16 g L-glutamine and 1.10 g sodium pyruvate in 100 mL PBS)). The cell suspension was transferred into a sterile 15 mL tube. After centrifugation at 800 rcf for 5 min, the supernatant was aspirated and 1 mL of RBC lysis buffer Hybri-MaxTM (Sigma-Aldrich) was added for 1 min. The cell suspension was then quenched by adding 9 mL of T cell medium and filtered through 70 μ nylon mesh in a new 15 mL tube. The washing step was repeated twice and the suspension was ready for the desired cell separation.

Bone marrow-derived dendritic cell (BMDC) preparation

BMDCs were prepared according to the procedure of Matheu [50]. Briefly, the femur and tibia were separated, cleaned, and flushed out into T cell medium. The cells were cleared of RBC and suspended in T-cell medium at 10^6 cells mL^{-1} in a 25 cm^2 T25 flask (Corning Inc., Corning, NY, USA). Granulocyte macrophage-colony stimulating factor (GM-CSF) (Peprotech Inc.) at 100 U mL^{-1} (10ng mL^{-1}) and interleukin-4 (IL-4) (Peprotech Inc.) at 10 ng mL^{-1} were added to the culture at day 0. At day 3, 75% of the cell medium was transferred to a sterile 15 mL tube without disturbing the culture. The tube was then centrifuged at 600 rcf for 5 min; the supernatant was aspirated and the cell pellet was resuspended in fresh T-cell medium containing GM-CSF and IL-4, each at 10 ng mL^{-1}. This cell suspension was added back into the old flask. During days 6-10, DCs were harvested from the supernatant, centrifuged at 600 rcf for 5 min, and suspended in T-cell medium. The harvested DCs were counted and kept on ice until used.

CD4+ T cell proliferation assay

Two mice from each group were sacrificed on the 7th day after the second vaccine boost and antibody injection. A spleen cell suspension was prepared as described earlier. From the spleen cell suspension, CD4+ T cells were positively isolated using a Dynabeads Flowcomp Mouse CD4 kit (Invitrogen). The remaining cell suspension was kept separately for CD8+ T cells for a future experiment. First, 90 μl of DC (2 x 10^4 cells) were added to each well and 60 μl of MUC1-Tn antigen was added per well in different concentrations (20, 2, 0.2, 0 μg mL^{-1}) and incubated for 30 minutes. Then 50 μl of CD4+ T cells (2 x 10^5 cells) from the different groups were added into their individual wells. Thus, the DC to CD4+ T cell ratio was 1:10. Cells were incubated for 72 hours at 37˚C and 5% CO_2. [^{3}H]-thymidine was then added at 40 μCi mL^{-1} and cells were harvested the next day on a glass-fiber filter plate. After drying the plate overnight, 40 μl of scintillation fluid was added in each well and thymidine incorporation was measured on a Top Count scintillation counter. For determining CD4+ T cell proliferation in the case of Rha-Ova, ratios of DC to CD4+ T cells were kept at 1:2.

CD8+ T cell proliferation assay

After separating CD4+ T cells, CD8+ T cells were positively separated using Dynabeads Flowcomp Mouse CD8 kit (Invitrogen). First, 90 μl of DCs (1 x 10^4 cells) were added to each well and 60 μl of CD8+ T cell epitope [35] was added per well at different concentrations (40, 4,

0.4, 0 μg/mL) and incubated for 30 minutes. Then 50 μl of CD8+ T cells (1 x 10^5 cells) from the different groups were added into their respective wells. Thus, the DC to CD8+ T cell ratio was 1:10. Cells were incubated for 72 hours at 37˚C and 5% CO_2. [^{3}H]-thymidine incorporation was measured as described above.

IFNγ production

Purified CD8+ T cells were distributed in a 12 well plate (5 x 10^5 cells in 500 μl per well). DCs (5 x 10^4 cells per well) cultured from bone marrow of a non-immunized mouse were mixed together with the CD8+ T cells to make a ratio of 1:10 (total volume of 1 mL). The combination of CD8+ T cells and DCs were pulsed with the CD8+ T cell epitope and incubated for 24 hours at 37˚C and 5% CO_2. The next day, the cell suspensions were centrifuged at 800 rcf and the supernatant collected immediately. IFNγ production was measured using a murine IFNγ ELISA kit (Peprotech).

Cytotoxicity assay

CD8+ T cells were isolated as discussed earlier. Cytotoxicity was determined using a JAM assay [51]. The EL4 lymphoma cell used as the target cell line was grown in RPMI 1640 media with 10% FBS. The day before the experiment, EL4 cells were split into 1 x 10^5 cells mL^{-1} in a T25 flask. The next day, [^{3}H]-thymidine was added and incubated at 37˚C and 5% CO_2 for 4 hr. After washing, the EL4 cell concentration was brought into 1 x 10^4 cells mL^{-1} and divided into two equal halves. One half was pulsed with CD8+ T cell epitope and incubated for 12 hours at 37˚C. Both targets were then washed twice, brought back to 1 x 10^5 cells mL^{-1}, and 100 μl was added into each well. The CD8+ T cell concentration was maintained at 1 x 10^6 cells mL^{-1} and 100 μl was added into each well. The EL4 cells alone and EL4 cells with CD8+ T cell epitope acted as the negative control groups whereas 100 μl of 2 μM staurosporine (Sigma-Aldrich) was used as a positive control group. The plate was incubated for 6 hours at 37˚C and 5% CO_2. The cells were then harvested on a glass-fiber filter plate. After drying the plate overnight, 40 μl of scintillation fluid was added in each well and thymidine incorporation was measured on a Top Count scintillation counter (Packard, Downers Gove). Cytotoxicity was determined using the following formula:

% Specific cytotoxicity = % cytotoxicity of peptide pulsed EL4 – % cytotoxicity of unpulsed EL4.

$$\% \text{ Cytotoxicity} = \frac{\text{Spontaneous killing (CPM) - Experimental killing (CPM)}}{\text{Spontaneous killing (CPM)}}$$

Spontaneous killing reflects the cpm value of EL4 cells alone and experimental killing reflects the cpm value of EL4 + CD8+ T cells. Cytotoxicity of staurosporine was considered as 100% and % specific cytotoxicity was calculated accordingly.

Statistical analysis

Results are obtained as mean ± SD and significance was tested using one way or two way analysis of variance (ANOVA). For the proliferation assays and jam assay, Tukey's multiple comparison tests were performed. Statistical analysis was performed using Graph pad prism 7 software (**P < 0.01, ***P < 0.001, ****P < 0.0001).

Experimental Procedures for synthesis of Pam_3CysSK_4 -DBCO-MUC1 VNTR-TACA conjugate (9)

General methods

2-Chlorotrityl chloride resin was obtained from Chempep. Amino acids and HOBt were purchased from Chem-Impex International. All other fine chemicals were from one of the suppliers: Acros Organics, Alfa Aesar, Fisher Scientific, and Sigma-Aldrich. Flash column chromatography was done on silica gel (230-400 mesh) obtained from Sorbent Technologies using solvents as received. ^{1}H NMR and ^{13}C NMR were recorded on an AVANCE 600 MHz spectrometer in $CDCl_3$ using residual $CHCl_3$ as an internal reference.

Synthesis of Pam_3Cys *tert*-butyl ester (2)

O-palmitoylated Fmoc L-cystine *tert*-butyl ester [41] (1.55 g, 1.63 mmol) was dissolved in a mixture of acetonitrile:DCM:diethylamine (2:1:2, 10 mL) and stirred under N_2 atmosphere at room temperature. Complete Fmoc deprotection was observed on TLC (hexane: EtOAc, 4:1) after 2h. The reaction mixture was evaporated to dryness. Palmitic acid (0.5 gm, 1.95 mmol), PyBOP (1.02 g, 1.95 mmol) and HOBt (264 mg, 1.95 mmol) were dissolved in DCM (20 mL) followed by addition of DIPEA. The reaction mixture was stirred for 10 mins and added to the deprotected compound. The mixture was stirred under N_2 atmosphere at RT and observed to be complete after 5h on TLC (hexane: EtOAc, 4:1). The crude residue obtained after evaporation of the reaction mixture was purified using silica gel column chromatography using hexane: EtOAc as a solvent system to obtain **2** as a white solid (1.02 g, 71%). ^{1}H NMR (600 MHz, $CDCl_3$): δ 0.89 (t, 9H, J = 12 Hz Pam-CH_3), 1.26-1.65 (m, 78 H, Pam-CH_2), 1.51 (s, 9H, O*t*Bu-CH_3), 2.24-2.34 (m, 6H, J = 6 Hz, $COCH_2$), 2.74 (m, 2H, J = 6 Hz, S-CH_2), 3.03 (dd, 2H, J = 6 Hz, S-CH_2), 4.12 and 4.32 (dd, 2H, J = 12 Hz, CH_2-OPam), 4.71 (m, 1 H, J = 12 Hz, CH-NH), 5.15 (m, 1H, CH-OPam), 6.30 (d, 1H, J = 8.4 Hz, Pam-NH). ^{13}C NMR (600 MHz, $CDCl_3$): δ 14-37 (50 C), 52.35, 63.48, 70.30, 82.87, 169.66, 172.92, 173.06, 173.32. ESI-MS [M + Na] *m/z*: calcd for $C_{58}H_{111}NNaO_7S$, 988.8; found, 988.6.

Synthesis of Pam_3Cys carboxylic acid (3)

Pam_3Cys tertiary butyl ester **2** (1.02 g) was dissolved in a mixture of DCM:TFA (1:1, 4 mL) and stirred under N_2 at RT. Complete deprotection was observed on TLC (hexane:EtOAc, 4:1) after 1h. The solvent was evaporated on a rotary evaporator. DCM:toluene (1:1, 4 mL) mixture was added to the residue multiple times and evaporated to ensure complete removal of TFA and afford compound **3** as a pale white solid (927 mg, quantitative). ^{1}H NMR (600 MHz, $CDCl_3$): δ 0.89 (t, 9H, J = 12 Hz Pam-CH_3), 1.26-1.65 (m, 78 H, Pam-CH_2), 2.24-2.34 (m, 6H, J = 6 Hz, $COCH_2$), 2.74 (m, 2H, J = 6 Hz, S-CH_2), 3.03 (dd, 2H, J = 6 Hz, S-CH_2), 4.12 and 4.32 (dd, 2H,

J = 12 Hz, CH_2-OPam), 4.71 (m, 1 H, J = 12 Hz, CH-NH), 5.15 (m, 1H, CH-OPam), 6.30 (d, 1H, J = 8.4 Hz, Pam-NH). ^{13}C NMR (600 MHz, $CDCl_3$): δ 14-37 (47 C), 51.9, 63.7, 70.20, 172.46, 173.56, 173.64, 174.43. ESI-MS [M + H] *m/z*: calcd for $C_{54}H_{103}NO_7S$, 910.7; found, 910.6.

Synthesis of Pam_3CysSK_4 (5)

Pam_3CysSK_4 was synthesized by a Fmoc strategy using solid phase chemistry (Scheme **2**). The resin beads (0.5 g) were soaked in DCM (10 mL) overnight. A syringe was used for SPPS, the bottom of which was closed with a filter. The first amino acid residue N_α-Fmoc-N_ε-Boc-L-lysine (1.1 equi.) was loaded on the resin in presence of DIPEA (5 equi.) for 4 h followed by end group capping with methanol for 20 min. A continuous stream of N_2 was bubbled from the bottom to agitate the mixture of beads and reagents. The resin beads were washed successively with DCM, DMF, and methanol. Fmoc deprotection was achieved using 25 % piperidine in DMF (4 mL) in 30 mins and coupling was performed using DIC (1.5 equi.), HOBt (1.5 equi.) and Fmoc amino acid (1.5 equi.). The reaction was monitored using the ninhydrin test and appeared complete after 4.5 h. After every deprotection and coupling step, resin beads were washed successively with DCM and DMF. N_α-Fmoc-N_ε-Boc-L-lysine and Fmoc-*O*-*tert*-butyl-L-serine amino acids were used to obtain the SK_4 peptide bound to the resin according to SPPS protocol.

The final coupling was performed using compound **3** which was synthesized from *O*-palmitoylated Fmoc-L-cystine *tert*-butyl ester **1** (Scheme **1**). Compound **3** (750 mg, 0.825 mmol) was dissolved in a mixture of DCM:DMF (1:1, 4 mL) followed by HOBt (172 mg, 0.825 mmol) and DIC (180 µl, 0.825 mmol). The reaction solution was added to the SK_4 bound resin suspended in 2 mL of DCM. The resin was agitated for 5 h and the reaction appeared complete as monitored by the ninhydrin test. The beads were washed successively with DMF and DCM. The resin beads were suspended in an acetic acid:DCM solution (1:2, 6 mL) for 2 h and filtered. The mixture was evaporated on a rotary evaporator. A DCM:hexane (1:1, 4 mL) solution was added to the residue and evaporated. This procedure was repeated five times to afford compound **5** as a white solid (493 mg, 33%). MALDI-MS: [M+Na] *m/z* calcd for $C_{105}H_{196}N_{10}NaO_{21}S$, 1989.82; found 1989.796.

Synthesis of side-chain protected Pam_3CysSK_4-DBCO conjugate (6)

Compound **5** (60 mg, 30 µmol) and DBCO-amine (10 mg, 33 µmol) were dissolved in DCM (4 mL) followed by the addition of propyl phosphonic anhydride (T_3P) (27 µl, 45 µmol) and DIPEA (9 µl, 45 µmol). The solution was stirred under N_2 atmosphere at RT. The reaction was monitored by TLC ($CHCl_3$:EtOH) and appeared complete after 6.5 h. The reaction was diluted with DCM (5 mL) and washed with saturated $NaHCO_3$ (5 mL) and water (5 mL). The organic layer was separated, dried over anhydrous Na_2SO_4 and evaporated under reduced pressure. The residue was subjected to silica gel column chromatography ($CHCl_3$:EtOH) to obtain compound **6** as a white powder (33 mg, 50%). MALDI-MS: [M+Na] *m/z* calcd for $C_{123}H_{210}N_{12}NaO_{21}S$, 2248.160; found, 2248.899.

Synthesis of the glycopeptide (8)

Compound **6** (2.7 mg, 1.2 μmol) and azide terminated peptide **7** (2.7 mg, 1.2 μmol) were dissolved in a mixture of DCM:anhydrous MeOH (1:1, 1mL). The reaction was stirred under N_2 atmosphere at RT. Complete consumption of starting material was observed by MALDI after 12 h. The reaction mixture was concentrated. The residue was dissolved in $CHCl_3$ (3 mL) and washed with water (2 mL). The organic layer was dried over anhydrous Na_2SO_4 and evaporated under reduced pressure to obtain cyclo-addition product **8** as a pale yellow solid (5.2 mg, quantitative). MALDI-MS: [M+H] *m/z* calcd for $C_{217}H_{362}N_{41}O_{55}S$, 4457.488; found 4458.246.

Synthesis of Pam_3CysSK_4-DBCO-MUC1 VNTR-TACA conjugate (9)

The cyclo-addition product **8** (5.2 mg, 1.16 μmol) was dissolved in cleavage cocktail of DCM: TFA:TES (50:50:0.5, 1mL) and stirred for 40 min at RT under N_2 atmosphere. The DCM was evaporated and the remaining reaction mixture was added to cold ether (-10 °C, 5 mL). The solution was kept at -20 °C overnight for precipitation of the targeted compound. The precipitate was centrifuged, washed twice with cold ether, and dried under high vacuum to obtain compound **9** (4.4 mg, 91%). MALDI-MS: [M+H] *m/z* calcd for $C_{193}H_{320}N_{41}O_{47}S$, 3998.91; found 3998.65.

Supporting information

Supporting information consisting of Figure S1 and experimental characterization data (ESI-MS, NMR, and MALDI) of selected synthetic products is available online. This material is available free of charge via the internet at http://pubs.acs.org.

Conflict of interest statement

The authors declare no competing financial interest.

Acknowledgement

We would like to thank our previous lab member K. Kulkarni for his helpful discussion during the initial stage of the project. We would also like to thank S. Sarkar for his contribution towards synthesizing Rha-Ova. This work was supported by NIH 2R15-GM094734.

Author contributions

MKH prepared the Rha-affinity column, performed all the experiments related to biology and wrote the major portions of the manuscript. AV synthesized the liposomal vaccine and wrote that part of the paper. PK synthesized the linker for the Rha-affinity column. SJS and KW supervised, coordinated and directed the project.

References

1. Amanna, I. J., and Slifka, M. K. (2011) Contributions of humoral and cellular immunity to vaccine-induced protection in humans, *Virology 411*, 206-215.
2. Celluzzi, C. M., Mayordomo, J. I., Storkus, W. J., Lotze, M. T., and Falo, L. D., Jr. (1996) Peptide-pulsed dendritic cells induce antigen-specific CTL-mediated protective tumor immunity, *J Exp Med 183*, 283-287.
3. Banchereau, J., Briere, F., Caux, C., Davoust, J., Lebecque, S., Liu, Y. J., Pulendran, B., and Palucka, K. (2000) Immunobiology of dendritic cells, *Annu Rev Immunol 18*, 767-811.
4. Cruz, L. J., Rueda, F., Cordobilla, B., Simon, L., Hosta, L., Albericio, F., and Domingo, J. C. (2011) Targeting nanosystems to human DCs via Fc receptor as an effective strategy to deliver antigen for immunotherapy, *Mol Pharm 8*, 104-116.
5. Schmidt, J., Dojcinovic, D., Guillaume, P., and Luescher, I. (2013) Analysis, Isolation, and Activation of Antigen-Specific CD4(+) and CD8(+) T Cells by Soluble MHC-Peptide Complexes, *Front Immunol 4*, 218.
6. Amigorena, S., and Bonnerot, C. (1999) Fc receptors for IgG and antigen presentation on MHC class I and class II molecules, *Semin Immunol 11*, 385-390.
7. Berg, M., Uellner, R., and Langhorne, J. (1997) Fc gamma receptor II dependency of enhanced presentation of major histocompatibility complex class II peptides by a B cell lymphoma, *Eur J Immunol 27*, 1022-1028.
8. Gascoigne, N. R. J. (2008) Do T cells need endogenous peptides for activation?, *Nat Rev Immunol 8*, 895-900.
9. Pichichero, M. E. (2014) Challenges in vaccination of neonates, infants and young children, *Vaccine 32*, 3886-3894.
10. Akiyama, K., Ebihara, S., Yada, A., Matsumura, K., Aiba, S., Nukiwa, T., and Takai, T. (2003) Targeting apoptotic tumor cells to Fc gamma R provides efficient and versatile vaccination against tumors by dendritic cells, *J Immunol 170*, 1641-1648.
11. Swanson, J. A., and Hoppe, A. D. (2004) The coordination of signaling during Fc receptor-mediated phagocytosis, *J Leukoc Biol 76*, 1093-1103.
12. Schuurhuis, D. H., Ioan-Facsinay, A., Nagelkerken, B., van Schip, J. J., Sedlik, C., Melief, C. J., Verbeek, J. S., and Ossendorp, F. (2002) Antigen-antibody immune complexes empower dendritic cells to efficiently prime specific CD8+ CTL responses in vivo, *J Immunol 168*, 2240-2246.
13. Itzkowitz, S. H., Yuan, M., Montgomery, C. K., Kjeldsen, T., Takahashi, H. K., Bigbee, W. L., and Kim, Y. S. (1989) Expression of Tn, sialosyl-Tn, and T antigens in human colon cancer, *Cancer Res 49*, 197-204.
14. Livingston, P. O., Wong, G. Y., Adluri, S., Tao, Y., Padavan, M., Parente, R., Hanlon, C., Calves, M. J., Helling, F., Ritter, G., and et al. (1994) Improved survival in stage III melanoma patients with GM2 antibodies: a randomized trial of adjuvant vaccination with GM2 ganglioside, *J Clin Oncol 12*, 1036-1044.
15. Richichi, B., Thomas, B., Fiore, M., Bosco, R., Qureshi, H., Nativi, C., Renaudet, O., and BenMohamed, L. (2014) A cancer therapeutic vaccine based on clustered Tn-antigen mimetics induces strong antibody-mediated protective immunity, *Angew Chem Int Ed Engl 53*, 11917-11920.
16. Amon, R., Reuven, E. M., Leviatan Ben-Arye, S., and Padler-Karavani, V. (2014) Glycans in immune recognition and response, *Carbohydr Res 389*, 115-122.
17. Cao, Y., Karsten, U., Otto, G., and Bannasch, P. (1999) Expression of MUC1, Thomsen-Friedenreich antigen, Tn, sialosyl-Tn, and alpha2,6-linked sialic acid in hepatocellular carcinomas and preneoplastic hepatocellular lesions, *Virchows Arch 434*, 503-509.
18. Beatson, R., Maurstad, G., Picco, G., Arulappu, A., Coleman, J., Wandell, H. H., Clausen, H., Mandel, U., Taylor-Papadimitriou, J., Sletmoen, M., and Burchell, J. M. (2015) The Breast Cancer-

Associated Glycoforms of MUC1, MUC1-Tn and sialyl-Tn, Are Expressed in COSMC Wild-Type Cells and Bind the C-Type Lectin MGL, *PLoS One 10*, e0125994.
19. Munkley, J. (2016) The Role of Sialyl-Tn in Cancer, *Int J Mol Sci 17*, 275.
20. Cazet, A., Julien, S., Bobowski, M., Burchell, J., and Delannoy, P. (2010) Tumour-associated carbohydrate antigens in breast cancer, *Breast Cancer Res 12*, 204.
21. Patton, S., Gendler, S. J., and Spicer, A. P. (1995) The epithelial mucin, MUC1, of milk, mammary gland and other tissues, *Biochim Biophys Acta 1241*, 407-423.
22. Hossain, M. K., and Wall, K. A. (2016) Immunological Evaluation of Recent MUC1 Glycopeptide Cancer Vaccines, *Vaccines (Basel) 4,* 25.
23. Guo, Z., and Wang, Q. (2009) Recent development in carbohydrate-based cancer vaccines, *Curr Opin Chem Biol 13*, 608-617.
24. Cai, H., Huang, Z. H., Shi, L., Sun, Z. Y., Zhao, Y. F., Kunz, H., and Li, Y. M. (2012) Variation of the glycosylation pattern in MUC1 glycopeptide BSA vaccines and its influence on the immune response, *Angew Chem Int Ed Engl 51*, 1719-1723.
25. Zhang, S., Graeber, L. A., Helling, F., Ragupathi, G., Adluri, S., Lloyd, K. O., and Livingston, P. O. (1996) Augmenting the immunogenicity of synthetic MUC1 peptide vaccines in mice, *Cancer Res 56*, 3315-3319.
26. Kagan, E., Ragupathi, G., Yi, S. S., Reis, C. A., Gildersleeve, J., Kahne, D., Clausen, H., Danishefsky, S. J., and Livingston, P. O. (2005) Comparison of antigen constructs and carrier molecules for augmenting the immunogenicity of the monosaccharide epithelial cancer antigen Tn, *Cancer Immunol Immunother 54*, 424-430.
27. Schutze, M. P., Leclerc, C., Jolivet, M., Audibert, F., and Chedid, L. (1985) Carrier-induced epitopic suppression, a major issue for future synthetic vaccines, *J Immunol 135*, 2319-2322.
28. Temizoz, B., Kuroda, E., and Ishii, K. J. (2016) Vaccine adjuvants as potential cancer immunotherapeutics, *Int Immunol 28*, 329-338.
29. Panda, S., and Ding, J. L. (2015) Natural antibodies bridge innate and adaptive immunity, *J Immunol 194*, 13-20.
30. Oyelaran, O., McShane, L. M., Dodd, L., and Gildersleeve, J. C. (2009) Profiling human serum antibodies with a carbohydrate antigen microarray, *J Proteome Res 8*, 4301-4310.
31. Sarkar, S., Lombardo, S. A., Herner, D. N., Talan, R. S., Wall, K. A., and Sucheck, S. J. (2010) Synthesis of a single-molecule L-rhamnose-containing three-component vaccine and evaluation of antigenicity in the presence of anti-L-rhamnose antibodies, *J Am Chem Soc 132*, 17236-17246.
32. Sheridan, R. T., Hudon, J., Hank, J. A., Sondel, P. M., and Kiessling, L. L. (2014) Rhamnose glycoconjugates for the recruitment of endogenous anti-carbohydrate antibodies to tumor cells, *Chembiochem 15*, 1393-1398.
33. Li, X., Rao, X., Cai, L., Liu, X., Wang, H., Wu, W., Zhu, C., Chen, M., Wang, P. G., and Yi, W. (2016) Targeting Tumor Cells by Natural Anti-Carbohydrate Antibodies Using Rhamnose-Functionalized Liposomes, *ACS Chem Biol 11*, 1205-1209.
34. Sarkar, S., Salyer, A. C., Wall, K. A., and Sucheck, S. J. (2013) Synthesis and immunological evaluation of a MUC1 glycopeptide incorporated into l-rhamnose displaying liposomes, *Bioconjug Chem 24*, 363-375.
35. Karmakar, P., Lee, K., Sarkar, S., Wall, K. A., and Sucheck, S. J. (2016) Synthesis of a Liposomal MUC1 Glycopeptide-Based Immunotherapeutic and Evaluation of the Effect of l-Rhamnose Targeting on Cellular Immune Responses, *Bioconjug Chem 27*, 110-120.
36. Abdel-Motal, U. M., Guay, H. M., Wigglesworth, K., Welsh, R. M., and Galili, U. (2007) Immunogenicity of influenza virus vaccine is increased by anti-gal-mediated targeting to antigen-presenting cells, *J Virol 81*, 9131-9141.

37. Galili, U. (2013) Anti-Gal: an abundant human natural antibody of multiple pathogeneses and clinical benefits, *Immunology 140*, 1-11.
38. Azuma, I., and Seya, T. (2001) Development of immunoadjuvants for immunotherapy of cancer, *Int Immunopharmacol 1*, 1249-1259.
39. Vogel, F. R. (1995) Immunologic adjuvants for modern vaccine formulations, *Ann N Y Acad Sci 754*, 153-160.
40. Funderburg, N. T., Jadlowsky, J. K., Lederman, M. M., Feng, Z., Weinberg, A., and Sieg, S. F. (2011) The Toll-like receptor 1/2 agonists Pam(3) CSK(4) and human beta-defensin-3 differentially induce interleukin-10 and nuclear factor-kappaB signalling patterns in human monocytes, *Immunology 134*, 151-160.
41. Metzger, J. W., Wiesmueller, K. H., and Jung, G. (1991) Synthesis of Nα-Fmoc protected derivatives of S-(2, 3-dihydroxypropyl)-cysteine and their application in peptide synthesis, *International journal of peptide and protein research 38*, 545-554.
42. Tel, J., Schreibelt, G., Sittig, S. P., Mathan, T. S., Buschow, S. I., Cruz, L. J., Lambeck, A. J., Figdor, C. G., and de Vries, I. J. (2013) Human plasmacytoid dendritic cells efficiently cross-present exogenous Ags to CD8+ T cells despite lower Ag uptake than myeloid dendritic cell subsets, *Blood 121*, 459-467.
43. Martinez, V., Ingwers, M., Smith, J., Glushka, J., Yang, T., and Bar-Peled, M. (2012) Biosynthesis of UDP-4-keto-6-deoxyglucose and UDP-rhamnose in pathogenic fungi Magnaporthe grisea and Botryotinia fuckeliana, *J Biol Chem 287*, 879-892.
44. Murelli, R. P., Zhang, A. X., Michel, J., Jorgensen, W. L., and Spiegel, D. A. (2009) Chemical control over immune recognition: a class of antibody-recruiting small molecules that target prostate cancer, *J Am Chem Soc 131*, 17090-17092.
45. Parker, C. G., Domaoal, R. A., Anderson, K. S., and Spiegel, D. A. (2009) An antibody-recruiting small molecule that targets HIV gp120, *J Am Chem Soc 131*, 16392-16394.
46. Surman, D. R., Dudley, M. E., Overwijk, W. W., and Restifo, N. P. (2000) Cutting edge: CD4+ T cell control of CD8+ T cell reactivity to a model tumor antigen, *J Immunol 164*, 562-565.
47. Ossendorp, F., Mengede, E., Camps, M., Filius, R., and Melief, C. J. (1998) Specific T helper cell requirement for optimal induction of cytotoxic T lymphocytes against major histocompatibility complex class II negative tumors, *J Exp Med 187*, 693-702.
48. Stager, S., Alexander, J., Kirby, A. C., Botto, M., Rooijen, N. V., Smith, D. F., Brombacher, F., and Kaye, P. M. (2003) Natural antibodies and complement are endogenous adjuvants for vaccine-induced CD8+ T-cell responses, *Nat Med 9*, 1287-1292.
49. Baumgarth, N., Tung, J. W., and Herzenberg, L. A. (2005) Inherent specificities in natural antibodies: a key to immune defense against pathogen invasion, *Springer Semin Immunopathol 26*, 347-362.
50. Matheu, M. P., Sen, D., Cahalan, M. D., and Parker, I. (2008) Generation of bone marrow derived murine dendritic cells for use in 2-photon imaging, *J Vis Exp 2008,* 773.
51. Matzinger, P. (1991) The JAM test. A simple assay for DNA fragmentation and cell death, *J Immunol Methods 145*, 185-192.

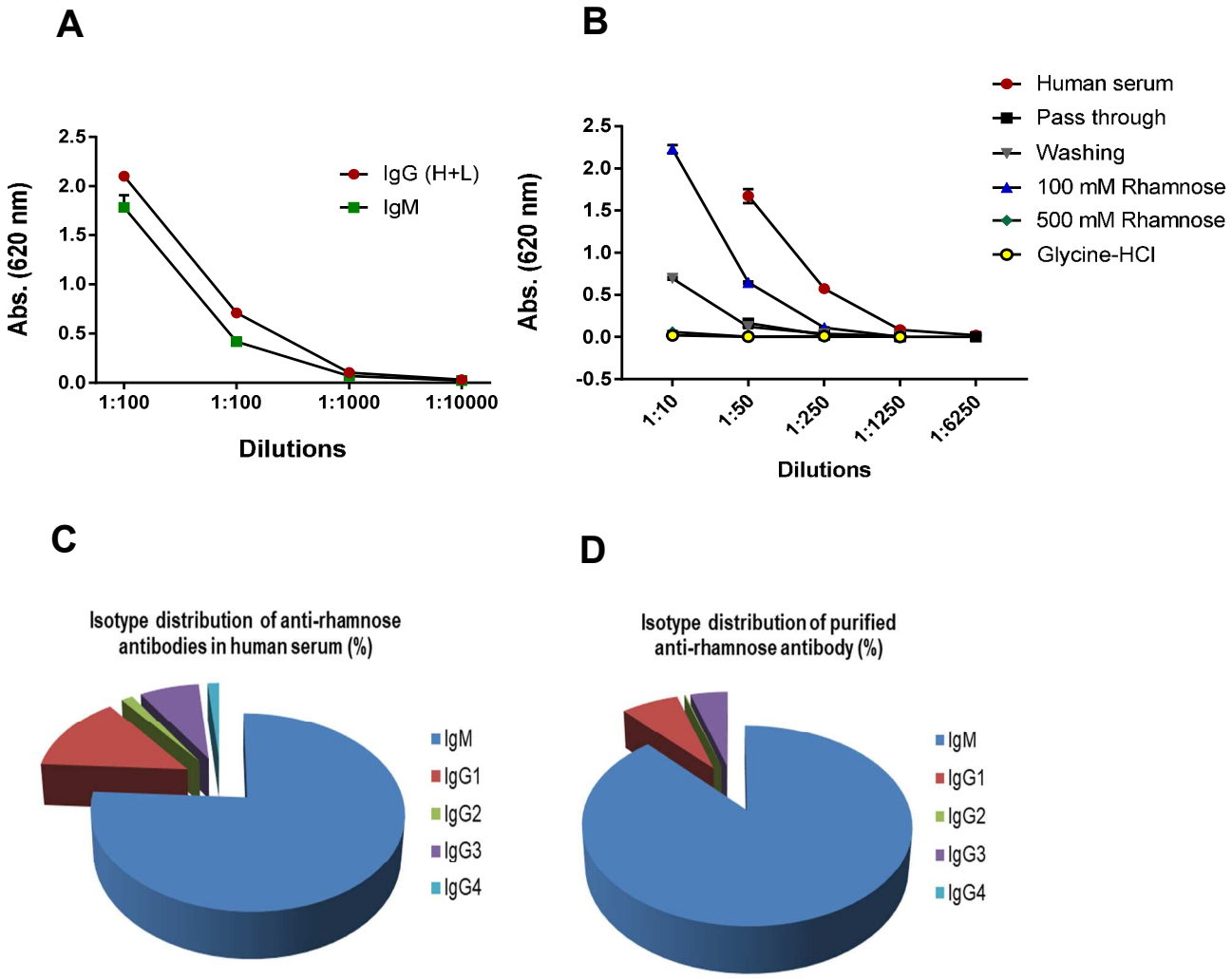

Fig.1. Purification and characterization of human anti-rhamnose antibodies.

A) Pooled human serum assayed with a Rha-specific ELISA to determine the concentration of anti-rhamnose antibody in serum. **B)** Rhamnose specific ELISA with different fractions from the affinity column showing the amount of anti-rhamnose antibodies in each. **C)** Natural anti-Rha antibodies found in human serum are mostly IgM, IgG1 and IgG3. **D)** Purified anti-Rha antibodies also reflect this distribution.

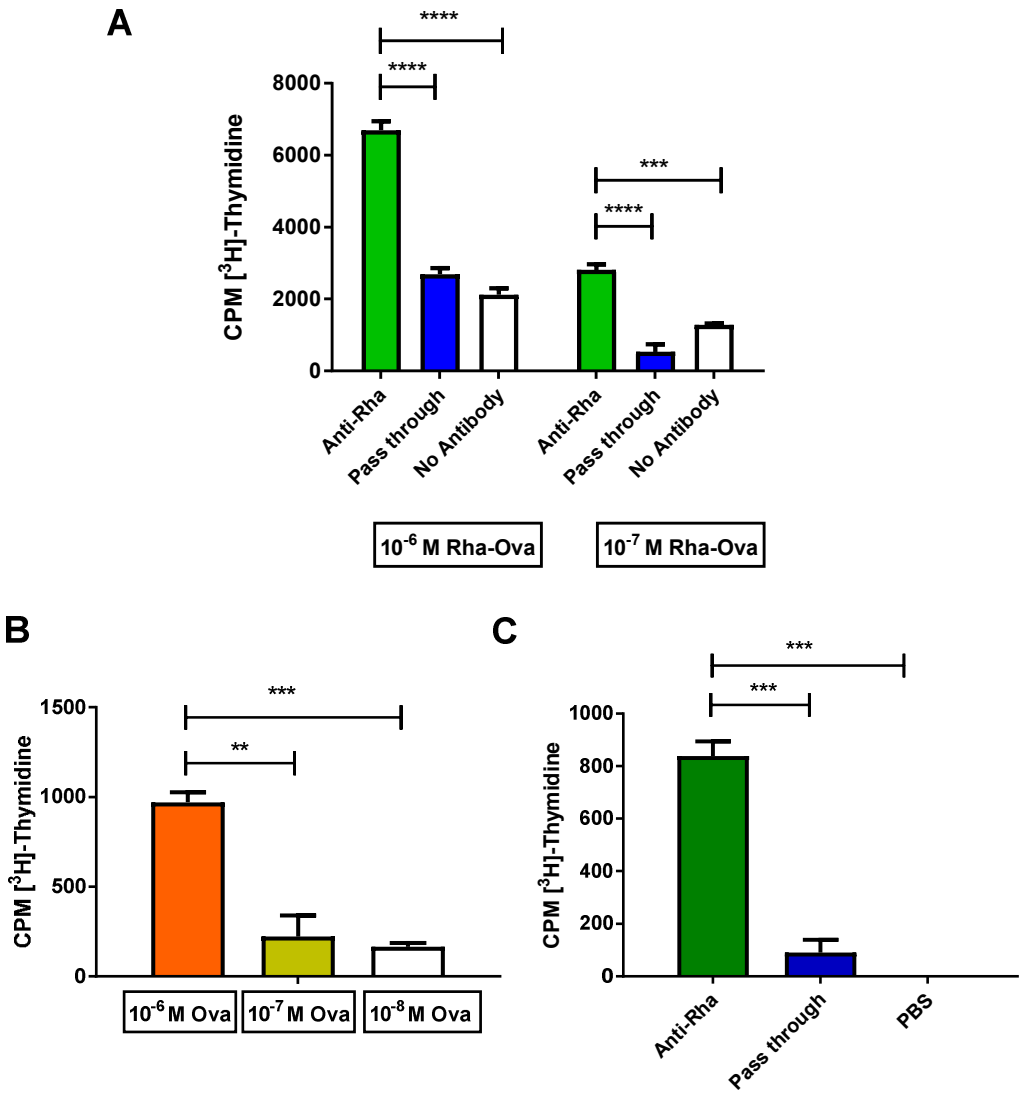

Fig.2. Human anti-rhamnose antibodies enhance antigen presentation and T cell priming.

A) *In vitro* proliferation assay with anti-Rha or pass through antibodies (Abs) added to DCs and Rha-ovalbumin (Rha-Ova), followed by Ova-primed CD4+ T cells. CPM value of PBS group was subtracted from experimental groups. **B)** *In vivo* priming: Determination of optimal Ova concentration for stimulation of CD4+ T cells from mice primed with Rha-Ova in the presence of anti-Rha Abs. Mice were injected with anti-Rha (10 µg) or pass through (10 µg) Abs and then Rha-Ova (40 µg). One week later, T cell priming was tested by stimulation of isolated T cells with DC and different concentrations of Ova *in vitro*. **C)** Proliferation to 10^{-6} M of Ova of T cells primed in the presence of anti-Rha Abs.

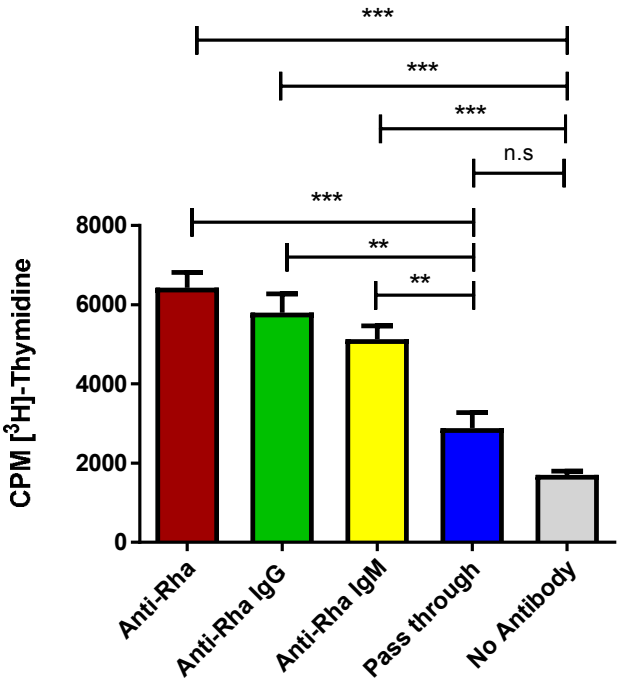

Fig. 3. Enhancement of antigen presentation by separated anti-rhamnose IgG and IgM.

In-vitro CD4+ T cell proliferation assays were performed to determine if the proliferative response of Ova-primed B6 CD4+ T cells was potentiated by mixing human anti-rhamnose antibodies or pass through (non-anti-Rha) with Rha-Ova and B6 dendritic cells as antigen-presenting cells.

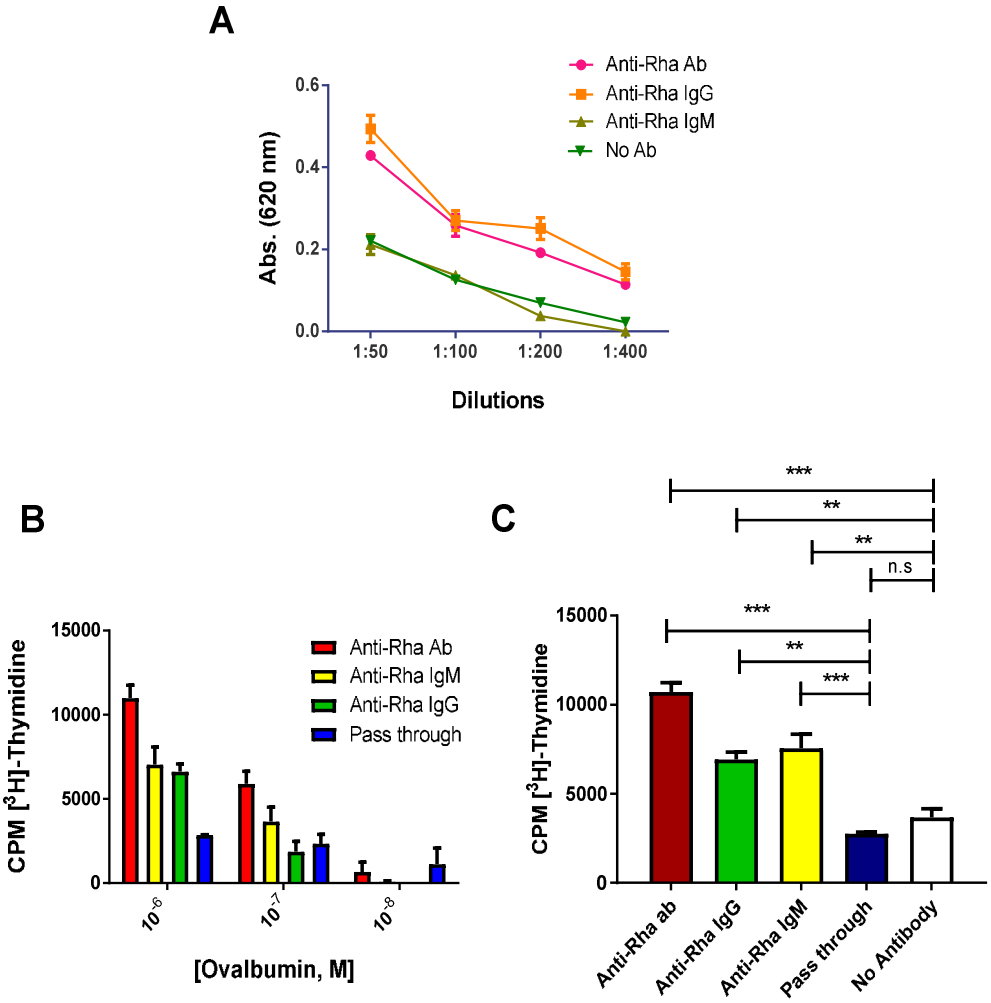

Fig. 4. *In vivo* enhancement by separated anti-rhamnose IgG and IgM.

CD4+ T cell help *in vivo* assays were performed. A) Mice were injected with different anti-Rha or pass through (10µg) Abs and Rha-Ova (40 µg). Serum collected one week later was assayed for anti-ovalbumin Abs. B) Concentration dependent proliferative response of T cells primed *in vivo* with Rha-Ova and different human Abs and assayed *in vitro* with Ova and DC. C) Data from (B) at 10^{-6} M Ova replotted with the no Ab control.

Scheme 1[a]. Synthesis of Pam_3Cys-OH.

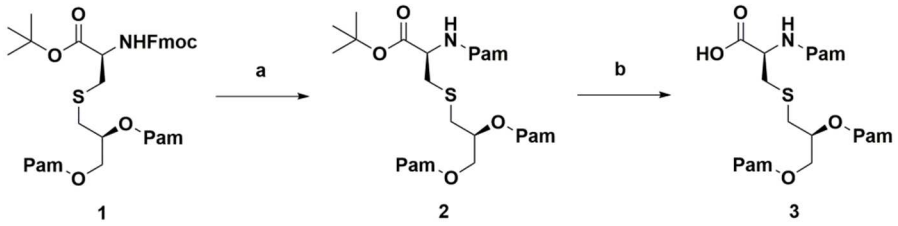

[a]Reagents and conditions: (a) (i) CH_3CN-CH_2Cl_2-Et_2NH (2:1:2), r.t., 2 h; (ii) PamOH, PyBOP, HOBt, DIPEA, CH_2Cl_2, r.t., 5 h, 71% (2 steps) [Pam = $CH_3(CH_2)_{14}CO$]. (b) TFA-DCM (1:1), r.t., 1 h, quantitative.

Scheme 2[a] : Synthesis of Pam_3CysSK_4-DBCO conjugate.

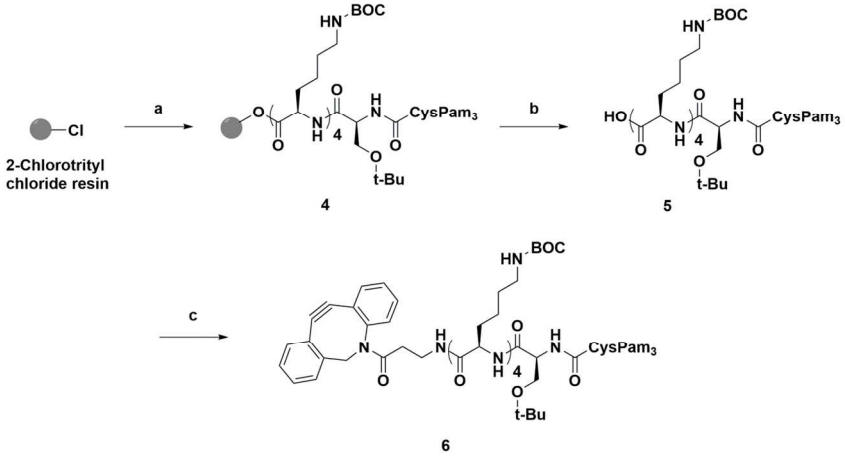

[a]Reagents and conditions: (a) (i) 25% piperidine, DMF, r.t. 30 min; (ii) HOBt, DIC, N_α-Fmoc-N_ε-Boc-L-lysine, repeat steps with K, K, K, S, 3; (b) Acetic acid-DCM (1:2), r.t., 2 h; (c) DBCO-amine, T_3P, DIPEA, DCM, r.t, 5 h, 73%.

Scheme 3[a] : Synthesis of Pam_3CysSK_4-DBCO-MUC-1 VNTR-TACA conjugate 9.

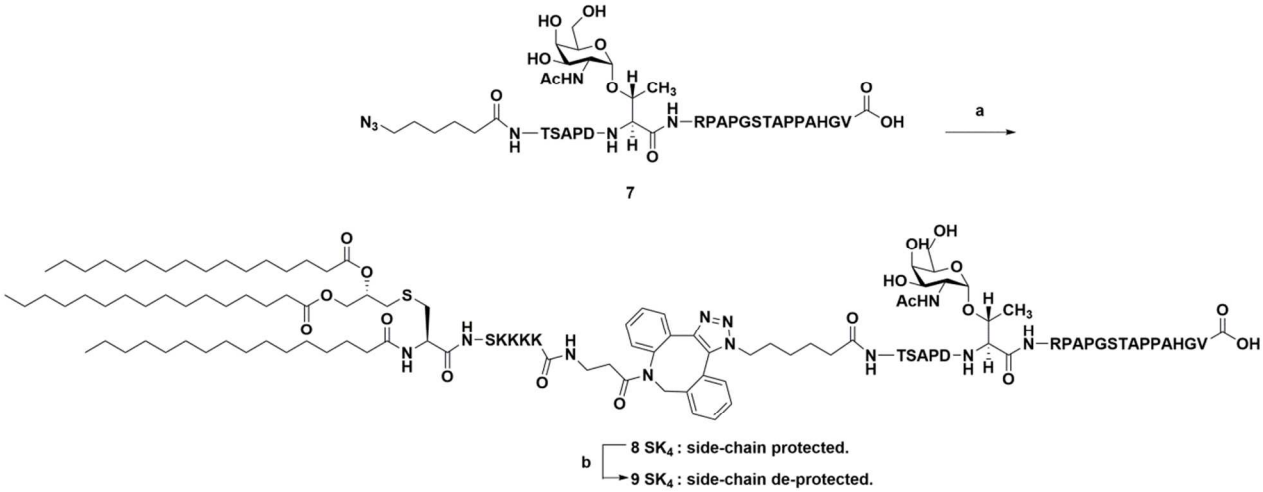

[a]Reagents and conditions : (a) **6**, MeOH - DCM (1:1), r.t, 12 h, quantitative; (b) DCM:TFA:TES (50:50:0.5), r.t, 40 min, 90.7 %.

Fig. 5. Synthesis of Pam_3CysSK_4-DBCO-MUC-1 VNTR-TACA

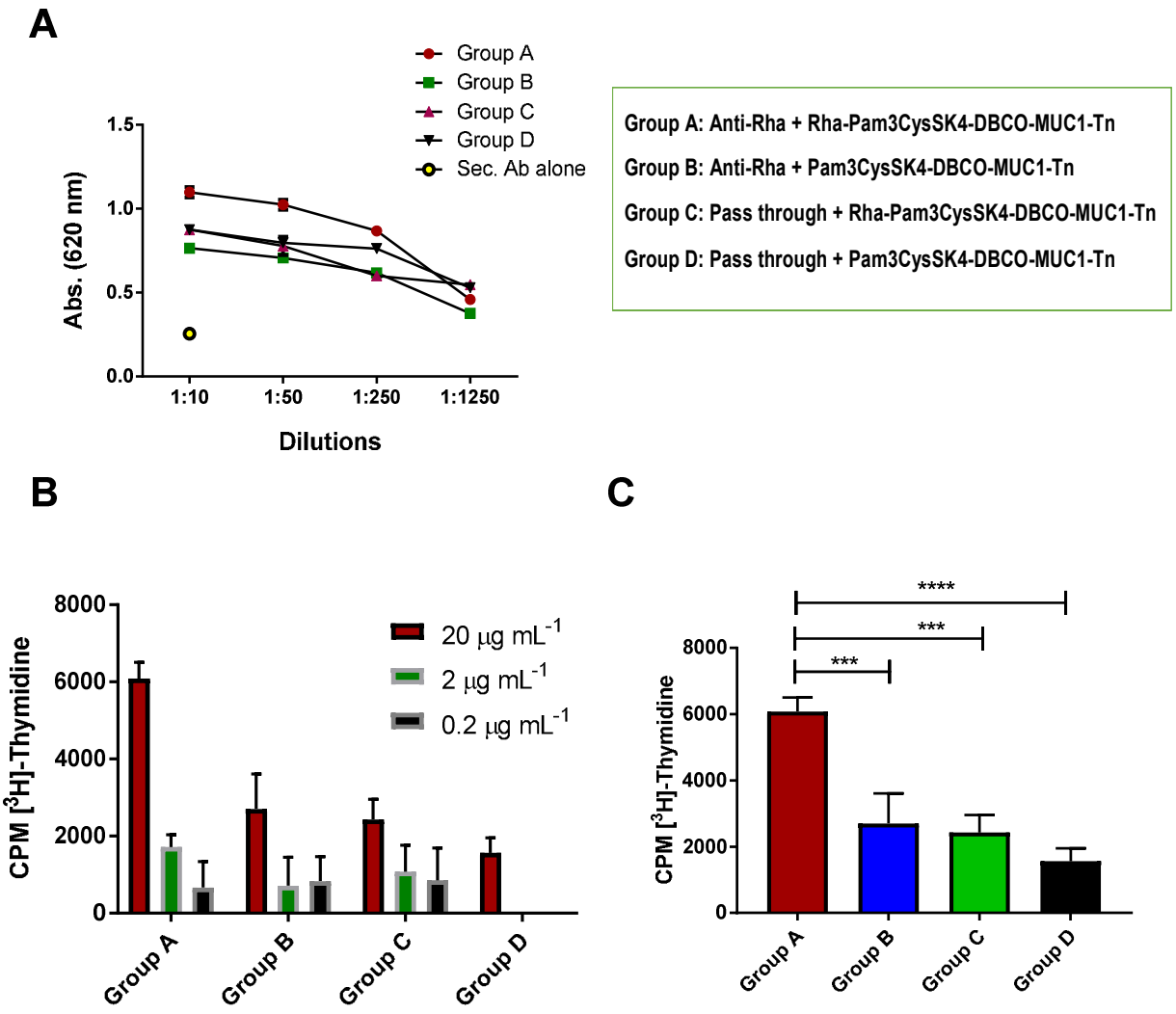

Fig. 6. *In vivo* enhancement of anti-MUC1-Tn response by human anti-rhamnose antibodies.

A) Mice were injected with anti-Rha or pass through Abs (10 μg) and one hour later immunized with MUC1-Tn antigen liposomes with or without Rhamnose. Sera were collected seven days after the second boost to measure MUC1-Tn antibody production. B) Concentration dependent and MUC1-Tn-specific CD4+ T cell proliferative response of the four different groups. The amounts refer to the concentration of MUC1-Tn present in each well. C) Data from B is plotted at 20 μg mL^{-1} concentration of MUC1-Tn. Control group and MUC1 non-specific proliferation was subtracted.

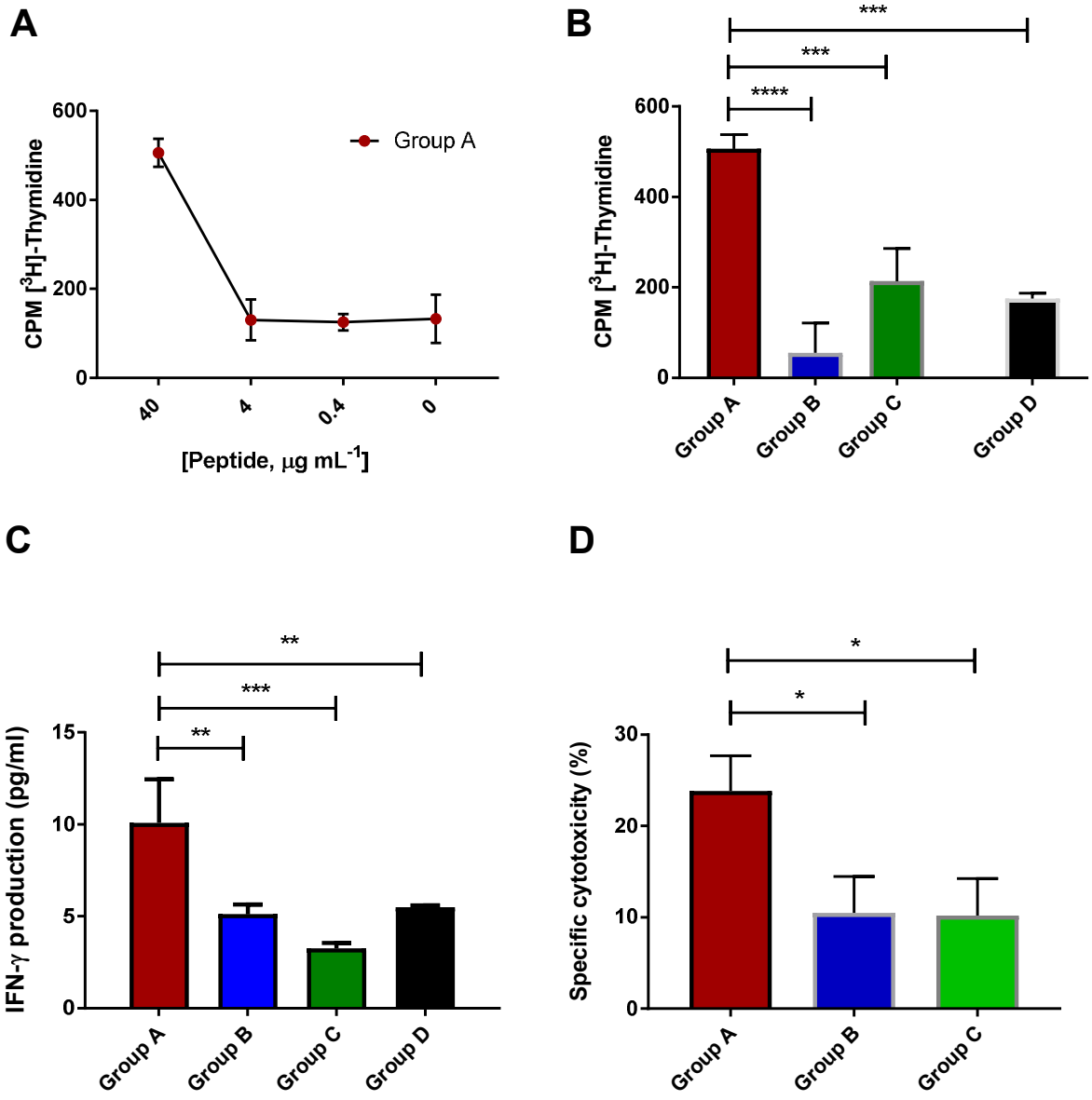

Fig. 7. Effect of human anti-rhamnose antibodies on CD8+ T cell responses to MUC1-Tn.

A) Concentration dependent CD8+ T cell proliferative response to MUC1-Tn peptide loaded DCs of group A. **B)** MUC1-specific CD8+ T cell proliferative response of the four different groups (40 µg mL^{-1}). Control group and MUC1-non-specific proliferation were subtracted. **C)** CD8+ T cell specific IFN-γ production in four groups of mice at 40 µg mL^{-1} CD8 MUC1-Tn epitope peptide. **D)** Apoptosis induced by CD8+ T cells of the different groups in EL4 cells presenting the CD8 epitope peptide. The ratio of EL4 to CD8+ cells was 1:100.

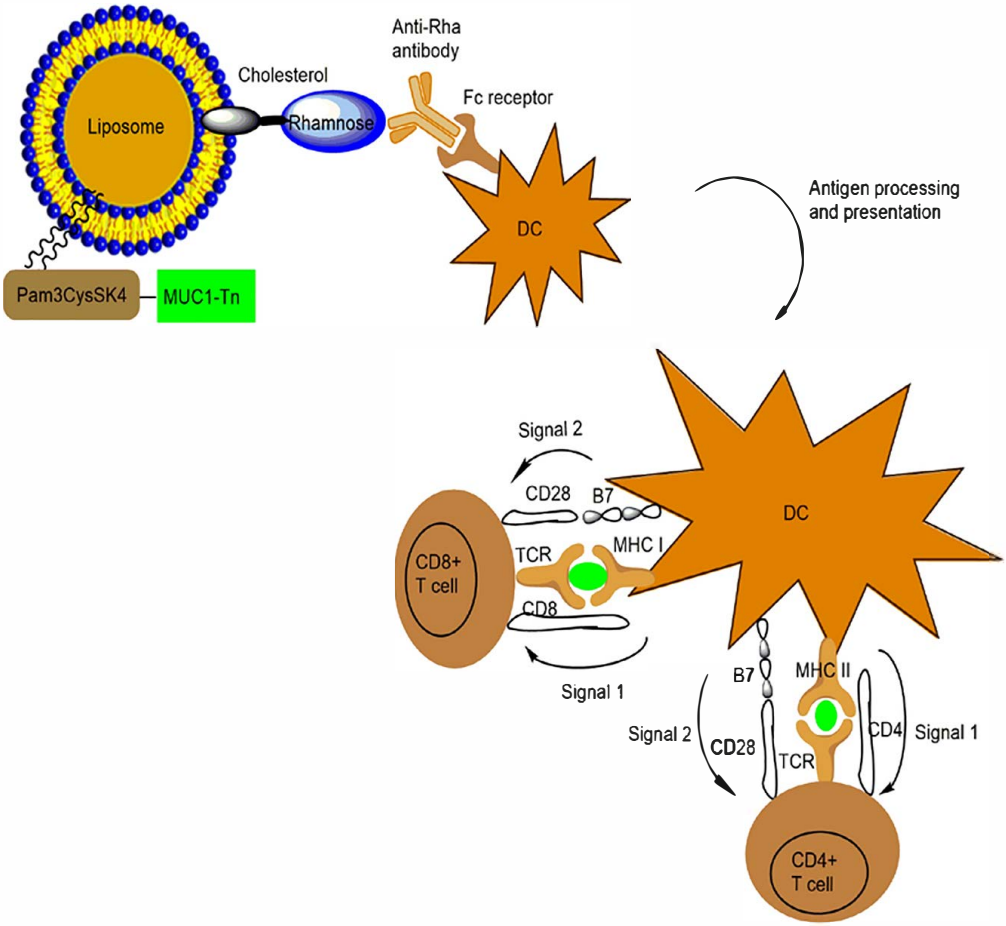
Liposome
Cholesterol
Rhamnose
Anti-Rha antibody
Fc receptor
DC
Antigen processing and presentation
Pam3CysSK4
MUC1-Tn
Signal 2
CD28
B7
DC
CD8+ T cell
TCR
MHC I
CD8
Signal 1
B7
MHC II
Signal 2
CD28
TCR
CD4
Signal 1
CD4+ T cell